Research Square

Preprints are preliminary reports that have not undergone peer review. They should not be considered conclusive, used to inform clinical practice, or referenced by the media as validated information.

Green Synthesis and Characterisation of Iron Oxide Nanoparticles Using Rice Husk and Orange Peel Extracts and Residue Templates (RHOPTNPs) for the Adsorptive Removal of Ciprofloxacin and Ibuprofen from Aqueous Solution

Habib Isa ADAMU

habibadamu99@kasu.edu.ng

Kaduna State University

Abdulrahman Abdulmumin Gbenga

University of Abuja

Muhammad-Najeeb Oluwafemi Yusuf

National Agency for Science and Engineering Infrastructure

Research Article

Keywords: Green synthesis, iron oxide nanoparticles, agricultural waste valorization, ciprofloxacin, ibuprofen, adsorption, rice husk, orange peel, pharmaceutical contaminants

Posted Date: October 6th, 2026

DOI: https://doi.org/10.21203/rs.3.rs-11040442/v1

License: This work is licensed under a Creative Commons Attribution 4.0 International License. Read Full License

Additional Declarations: No competing interests reported.

Green Synthesis and Characterisation of Iron Oxide Nanoparticles Using Rice Husk and Orange Peel Extracts and Residue Templates (RHOPTNPs) for the Adsorptive Removal of Ciprofloxacin and Ibuprofen from Aqueous Solution

Adamu, H.I.[1], Gbenga, A.A.[2], and Yusuf, M.N.O.[3]

[1]Department of Pure and Applied Chemistry, Kaduna State University Kaduna
[2]Department of Chemistry, Faculty of Science, University of Abuja, Gwagwalada, Nigeria
[3]Scientific Equipment Development Institute Minna, National Agency for Scientific and Engineering Infrastructure (NSENI), Nigeria

Corresponding author: habibadamu99@kasu.edu.ng
OCID: 0009-0001-2252-1718

Abstract

Pharmaceutical contamination of water bodies by antibiotics and anti-inflammatory drugs poses a growing environmental and public health concern, while, driving interest in low-cost, green-synthesized adsorbents. In this study, iron oxide (Fe_3O_4/Fe_2O_3) nanoparticles were synthesized via a green co-precipitation route using a combined extract and residue (template) of rice husk and orange peel, designated as RHOPTNPs, and evaluated for the removal of ciprofloxacin and ibuprofen from aqueous solution. Spectroscopic and microscopic characterization confirmed the formation of capped, cubic magnetite (Fe_3O_4) nanoparticles with a BET surface area of 846.28 m^2 g^{-1} and a pore volume of 0.6582 cm^3 g^{-1}. Batch adsorption experiments showed a maximum ciprofloxacin removal efficiency of 99.45% under optimized conditions that include; a dose of 80 mg, 40-minute contact time, pH 7, and a temperature of 320 K, while ibuprofen removal reached up to 92.21% under the same optimized conditions. Equilibrium and kinetic data fitted well to the Langmuir isotherm and pseudo-second-order kinetic models, thus, indicating a monolayer, chemisorption-driven adsorption. Thermodynamic analysis showed a spontaneous process that was endothermic and exothermic for ciprofloxacin and ibuprofen, respectively. RHOPTNPs retained good performance over repeated adsorption–desorption cycles and were effective in treating real hospital and domestic wastewater, hence, establishing their potential as a sustainable, low-cost adsorbent for pharmaceutical contaminants present in water.

Keywords: Green synthesis; iron oxide nanoparticles; agricultural waste valorization; ciprofloxacin; ibuprofen; adsorption; rice husk; orange peel; pharmaceutical contaminants

1.0 Introduction

Pharmaceutical residues in aquatic environments have emerged as important contaminants of concern because of their continuous release and biological activity at low concentrations. Antibiotics such as ciprofloxacin (CIP) and non-steroidal anti-inflammatory drugs such as ibuprofen (IBU) have been detected in wastewater, surface water, and groundwater, primarily due to domestic and hospital discharges, incomplete removal during conventional wastewater treatment, and inappropriate disposal of pharmaceutical products. Their abundant organic compositions have classified them under persistent organic pollutants (POPs) that may contribute to antimicrobial resistance, ecological disturbances, and potential risks to human health [1].

Conventional wastewater treatment processes, including coagulation-flocculation, chlorination, and biological treatment, are not basically designed for the efficient removal of pharmaceutical micropollutants. Hence, adsorption has attracted considerable interest because of its operational simplicity, versatility, and potential cost-effectiveness [2]. Iron oxide nanoparticles (IONPs) are particularly promising owing to their high specific surface area, tunable surface chemistry, and, for magnetic phases, the potential for straightforward magnetic recovery from treated water [2, 3].

The conventional synthesis of nanoparticles may involve hazardous chemicals, high energy requirements, and undesirable by-products. Green synthesis using plant-derived phytochemicals has been extensively studied and found to offer a more sustainable alternative, while the conversion of agricultural residues into functional nanomaterials may provide additional benefits through waste valorization and resource recovery [4-7]. In addition, recent studies have demonstrated the relative capabilities of rice husk- and citrus-derived materials for the synthesis of iron-based nanoparticles and pharmaceutical waste adsorption, thereby, highlighting the relevance of agricultural residues as sustainable nanoparticle precursors.

Despite these advances, most reported green synthesis routes have relied primarily on plant extracts as reducing, stabilizing, or capping agents [4]. The simultaneous use of combined agricultural-waste extracts and their retained insoluble biomass as a structural template has comparatively received less attention. Such a template-assisted route may influence nucleation and particle growth while introducing biomass-derived functional groups and modifying the surface and textural characteristics of the resulting nanomaterial. In addition, the practical application of nanoparticle-based adsorbents is often limited by difficulties in recovering and

regenerating the spent material and by the progressive loss of adsorption performance during repeated use. Magnetic iron oxide nanoparticles offer a direct solution to this limitation, as their magnetic responsiveness allows the spent adsorbent to be rapidly separated from treated water using an external magnet, rather than by filtration or centrifugation, thereby simplifying recovery and enabling repeated regeneration and reuse.

In this study, iron oxide nanoparticles were synthesized using a combined rice husk-orange peel aqueous extract with the retained biomass residue serving as a natural structural template. The resulting material, designated as RHOPTNPs, was characterized by using various scientific methods to check its light absorption, chemical bonds, particle size, shape, crystal structure, surface area, and weight changes when heated. Its adsorption performance toward CIP and IBU was systematically evaluated under varying adsorbent dosage, contact time, solution pH, initial pharmaceutical concentration, and temperature. Equilibrium, kinetic, and thermodynamic models were applied to elucidate the adsorption behaviour. The regeneration and reuse performance of RHOPTNPs over successive adsorption–desorption cycles, together with its performance in real hospital and domestic wastewater, was also evaluated to assess its practical applicability.

The study therefore aimed to develop and evaluate a waste-derived, template-assisted iron oxide nanomaterial for pharmaceutical-contaminant removal and to establish the relationships between its physicochemical properties and adsorption performance.

2.1 Materials and Reagents

Rice husk and orange peel were collected as agricultural waste and employed as biomass precursors and natural templates. Rice husk was obtained from a local rice milling factory in the Mando area of Kaduna metropolis, while orange peel was collected from the fruits market at Bakin Dogo, also within Kaduna metropolis. Both materials were transported to the laboratory in labelled polythene bags, rinsed thoroughly with distilled water to remove impurities, dried under ambient conditions, ground using an electric blender, and sieved through a 60 mm mesh to obtain fine particles suitable for nanoparticle synthesis [3].Iron (II) chloride tetrahydrate ($FeCl_2 \cdot 4H_2O$) and iron (III) chloride hexahydrate ($FeCl_3 \cdot 6H_2O$) that served as Fe^{2+} and Fe^{3+} precursors, respectively, were purchased from Merck, and Sodium hydroxide (NaOH) purchased from Loba Chemie was used for pH adjustment and precipitation. Hydrochloric acid (HCl, 37%; Merck), sodium nitrate ($NaNO_3$; M = 85.00 g mol^{-1}; Suvchem), and nitric acid (HNO_3, 70%; Alpha Chemika) were

employed for point of zero charge (pH_pzc) determination. Ciprofloxacin intravenous infusion BP of 200 mg/100 mL solution concentration, and ibuprofen tablets (200 mg; Ranbaxy) were selected as model pharmaceutical contaminants. Deionized water was used throughout, and all reagents were of analytical grade and applied without further purification.

Domestic wastewater samples were collected from three areas of Kaduna metropolis, and the selection is based on population density, as indicated in Figure 1. Samples were obtained using clean 1-L glass bottles at three source points along the drainage channels and transported to the laboratory in ice-bath containers for analysis.

On the other hand, hospital wastewater samples were collected from three healthcare facilities within Kaduna metropolis, as also indicated in Figure 1, Samples were similarly taken directly from discharge points using clean 1-L glass bottles and immediately transported to the laboratory in ice-bath containers for analysis.

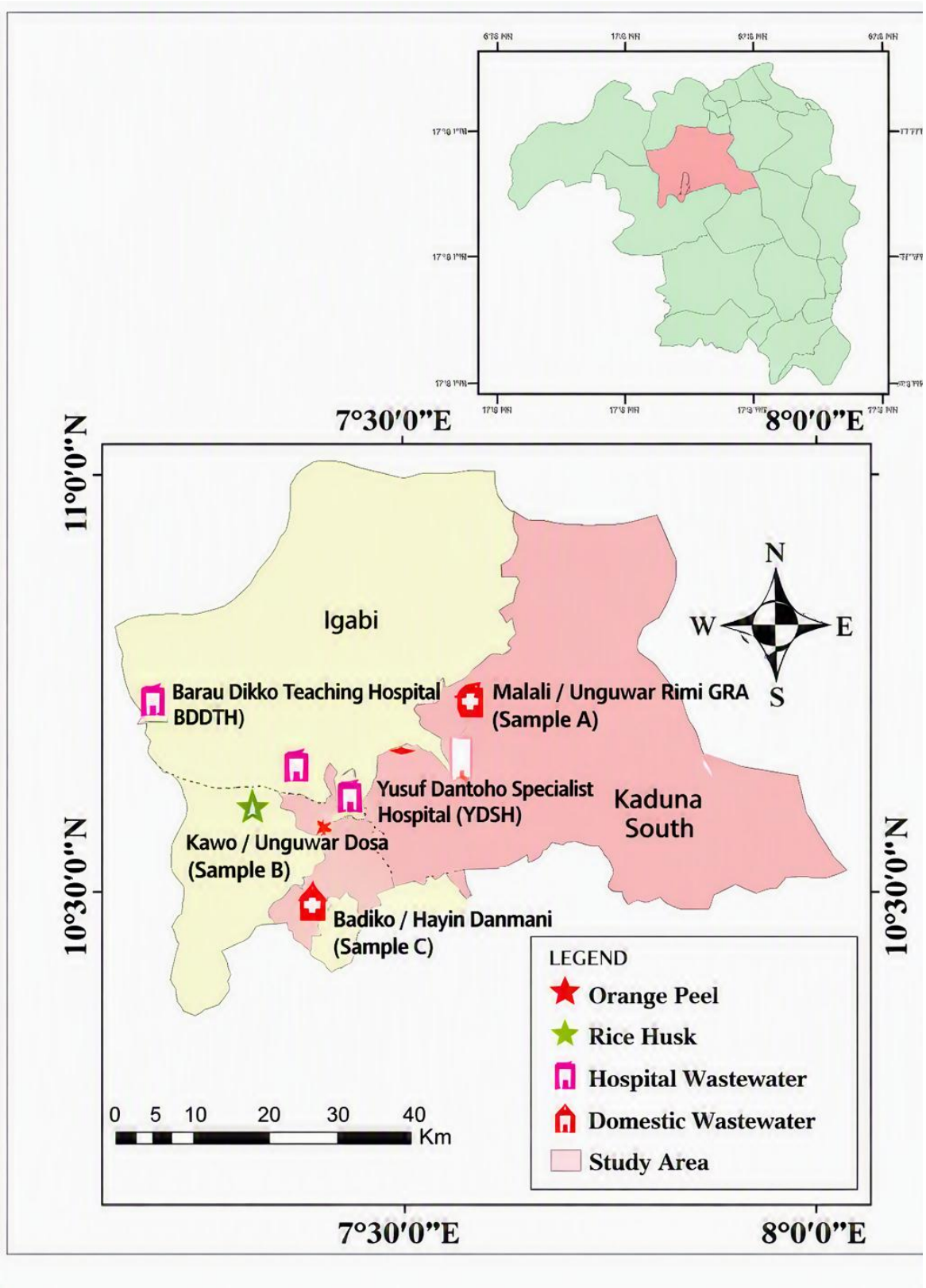

Figure 1: Map showing the sampling locations

2.2 Green Synthesis of Rice Husk–Orange Peel Templated Nanoparticles

Rice husk and orange peel were thoroughly washed with deionized water, sun-dried, pulverized separately and sieved. Equal masses were combined in a 1:1 ratio. Thirty grams of the mixture was dispersed in 200 mL of deionized water, heated at 40 °C for 15 min under continuous stirring at 500 rpm, and allowed to still for 4 h. The suspension was filtered through muslin cloth, and the retained fine biomass residues acted as a natural templating matrix during nanoparticle formation.

A 50 mL solution of Fe^{2+}/Fe^{3+} salts having molar ratio of 1:2 was gradually added to the extract–residue suspension under continuous stirring. The pH was adjusted to 11 using 1.0 M NaOH, and the mixture was stirred for 1 h at 500 rpm. Nanoparticle formation was indicated by the appearance of a dark blackish-brown colour. The product was recovered via centrifugation, washed four times with deionized water and once with ethanol, then dried at 130 °C for 24 h. The dried material was stored in an airtight container and designated RHOPTNPs (rice husk–orange peel templated nanoparticles).

2.3 Characterisation of RHOPTNPs

The physicochemical properties of RHOPTNPs were characterized using complementary analytical techniques. UV–visible spectroscopy in a range of 200–800 nm was employed to assess optical absorption characteristics. FTIR spectroscopy (4000–400 cm^{-1}) was used to identify functional groups associated with phytochemicals and nanoparticle stabilization.

Hydrodynamic particle size and polydispersity index were determined by dynamic light scattering (DLS). Surface morphology and elemental composition were examined using scanning electron microscopy coupled with energy-dispersive X-ray spectroscopy (SEM–EDS).

Crystalline phase and structural characteristics were analysed by X-ray diffraction (XRD) over a 2θ range of 10–80°, with average crystallite size estimated using the Scherrer equation where applicable.

Textural properties were determined from nitrogen adsorption–desorption measurements. Specific surface area was calculated using the Brunauer–Emmett–Teller (BET) method, while pore volume and pore-size distribution were derived from adsorption isotherms. The Langmuir surface area was also calculated for comparison [8].

Thermal stability and decomposition behaviour were evaluated by thermogravimetric analysis (TGA) under a controlled atmosphere at a specified heating rate (10°C min^{-1}) across the designated temperature range.

2.4 Batch Adsorption Experiments

Batch adsorption studies were conducted to evaluate the effects of adsorbent dosage, contact time, initial concentration, and solution pH on the removal of ciprofloxacin and ibuprofen by RHOPTNPs. All experiments were performed in triplicate.

2.4.1 Effect of Adsorbent Dosage and Contact Time

Fifty millilitres of ciprofloxacin or ibuprofen solution, having a concentration of 6.0 mg L^{-1}, and neutral pH were contacted with RHOPTNPs at dosages of ranging between 20–100 mg. Suspensions were agitated at 200 rpm in a temperature-controlled water-bath shaker. Aliquots were withdrawn at 5-min intervals over 40 min, filtered, and analysed spectrophotometrically. The dosage and contact time yielding maximum removal efficiency were selected as optimal conditions.

2.4.2 Effect of Initial Adsorbate Concentration

Solutions of ciprofloxacin and ibuprofen of concentration ranging between 2–10 mg L^{-1} were treated with RHOPTNPs with their optimized parameters. Residual concentrations were determined spectrophotometrically.

2.4.3 Effect of Solution pH

Pharmaceutical solutions were adjusted to pH ranging between 3–11 using 1.0 M HCl or NaOH (distinct from the 0.1 M HNO_3 used for the point-of-zero-charge titration in Section 2.5, which follows the salt-addition method of reference [9], then treated with RHOPTNPs under optimized conditions. Residual concentrations were measured spectrophotometrically, and the pH yielding maximum removal efficiency was identified as optimal.

Equilibrium adsorption capacity (q_e) and removal efficiency (R%) were calculated using Equations 1 and 2, respectively:

$$q_e = \frac{(C_0 - C_e)V}{m} \quad (1)$$

$$R(\%) = \frac{C_0 - C_e}{C_0} \times 100 \quad (2)$$

where and are the initial and equilibrium concentrations (mg L^{-1}), respectively; is solution volume (L); and is adsorbent mass (g).

2.4.4 Effect of Temperature

The effect of temperature on ciprofloxacin and ibuprofen removal by RHOPTNPs was investigated over the range 300–320 K, with the adsorbate solutions held at their respective optimized parameters and agitated at 200 rpm in a temperature-controlled water-bath shaker. Residual concentrations were determined spectrophotometrically and used to calculate q_e and R (%) by using Eqs. (1) and (2). The resulting equilibrium data were also used for the thermodynamic analysis described in Section 2.8.

2.5 Point of Zero Charge

The point of zero charge (pH_pzc) of RHOPTNPs was determined using the salt addition method [9]. 0.2 g of RHOPTNPs was added to 40 mL $NaNO_3$ solutions (0.05 and 0.10 M). The initial pH (pH_i) was adjusted between 2 and 11 using 0.1 M HNO_3 or NaOH. Suspensions were agitated at 200 rpm for 24 h, equilibrated, and the final pH (pH_f) was measured.

$$\Delta pH = pH_f - pH_i \quad (3)$$

A plot of ΔpH versus pH_i was used to determine pH_pzc at the intersection with ΔpH = 0.

2.6 Adsorption Isotherm Models

Equilibrium data were fitted to Langmuir, Freundlich, and Temkin isotherm models.

Langmuir model (monolayer adsorption):

$$\frac{C_e}{q_e} = \frac{1}{q_{\max} K_L} + \frac{C_e}{q_{\max}} \quad (4)$$

Separation factor:

$$R_L = \frac{1}{1+K_L C_0} \quad (5)$$

Freundlich model (heterogeneous surfaces):

$$\log q_e = \log K_F + \frac{1}{n} \log C_e \quad (6)$$

Temkin model (adsorbate–adsorbent interactions):

$$q_e = B_T \ln K_T + B_T \ln C_e \quad (7)$$

with

$$B_T = \frac{RT}{b_T} \quad (8)$$

Model suitability was assessed using R^2 values and consistency with experimental data.

2.7 Adsorption Kinetic Models

Kinetics were evaluated using pseudo-first-order, pseudo-second-order, intraparticle diffusion, and Elovich models.

Pseudo-first-order:

$$\ln(q_e - q_t) = \ln q_e - k_1 t \quad (9)$$

Pseudo-second-order:

$$\frac{t}{q_t} = \frac{1}{k_2 q_e^2} + \frac{t}{q_e} \quad (10)$$

Initial adsorption rate:

$$h = k_2 q_e^2 \quad (11)$$

Intraparticle diffusion (Weber–Morris model):

$$q_t = k_{id} t^{1/2} + C \quad (12)$$ [10].

Elovich model:

$$q_t = \frac{1}{\beta}\ln(\alpha\beta) + \frac{1}{\beta}\ln t \quad (13)$$

where q_e and q_t are the amounts of ciprofloxacin or ibuprofen adsorbed (mg g^{-1}) at equilibrium and at time t (min), respectively; k_1 (min^{-1}) and k_2 (g mg^{-1} min^{-1}) are the pseudo-first-order and pseudo-second-order rate constants, respectively; h (mg g^{-1} min^{-1}) is the initial adsorption rate; k_{id} (mg g^{-1} $min^{-1/2}$) is the intraparticle diffusion rate constant and C (mg g^{-1}) is the intercept related to boundary-layer thickness; and α (mg g^{-1} min^{-1}) and β (g mg^{-1}) are the initial adsorption rate and desorption-related constants of the Elovich model, respectively.

Model validity was assessed using R^2 values and agreement with experimental data.

2.8 Adsorption Thermodynamics

Thermodynamic parameters were evaluated at 300–320 K. Gibbs free energy change:

$$\Delta G^\circ = -RT \ln K_c \quad (14)$$

Van't Hoff equation:

$$\ln K_c = -\frac{\Delta H^\circ}{RT} + \frac{\Delta S^\circ}{R} \quad (15)$$

Negative ΔG° values indicated spontaneous adsorption, while ΔH° and ΔS° provided insights into adsorption nature and interfacial randomness.

2.9 Adsorbent Reusability

RHOPTNPs were regenerated and reused through successive adsorption–desorption cycles under optimized conditions. Adsorption performance retention was used to assess regeneration efficiency and stability, following approaches similar to Fe/Ni-MOF systems [11].

2.10 Application to Real Wastewater Samples

Domestic and hospital wastewater samples were collected, refrigerated, and analysed. Ciprofloxacin and ibuprofen concentrations were determined using calibration curves. Samples were treated with RHOPTNPs under optimized conditions, and removal efficiency was calculated,

as previously explained using Eq. (2). Results were compared with synthetic solutions to assess matrix effects.

3.0 Results and Discussion

3.1 Characterisation of RHOPTNPs

3.1.1 UV-Vis analysis

Formation of RHOPTNPs was first indicated by a colour change of the reaction mixture from brown to blackish-brown upon addition of the iron precursors and alkaline treatment, and confirmed by UV–Vis spectroscopy (Fig. 1). There was a visible distinct absorption band at ~305 nm that could be attributable to electronic transitions in the iron oxide phase and surface-bound phytochemicals from the rice husk–orange peel extract. This is found to be consistent with previously reported green-synthesized iron oxide nanoparticles [12].

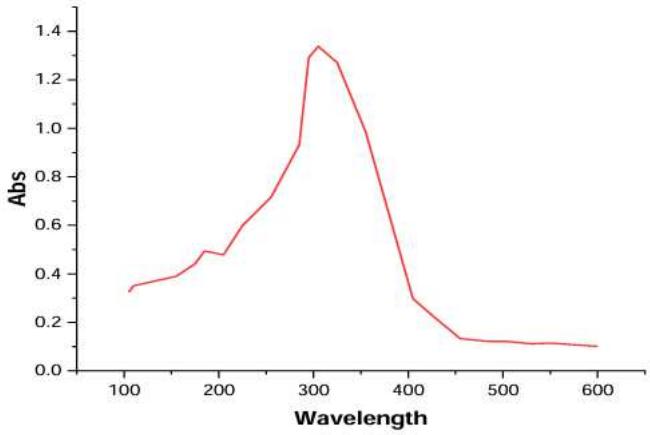

Figure 1. UV-Vis spectrum of RHOPTNPs

3.1.2 FTIR Analysis

The FTIR spectrum of RHOPTNPs, as shown in Fig. 2 exhibited absorption bands corresponding to both biomass-derived functional groups and the iron oxide phase. The bands observed at 3615–3876 cm^{-1} were assigned to O–H stretching vibrations of hydroxyl groups, while the band at 1498

cm^{-1} was attributed to aromatic C=C stretching associated with lignin- and polyphenol-derived structures. The absorption bands within 1073–1170 cm^{-1} were assigned to C–O stretching vibrations of oxygen-containing organic groups. A band at approximately 708 cm^{-1} was attributed to Fe–O vibrations, thus, providing evidence for the formation of the iron oxide phase.

The coexistence of organic and Fe–O bands indicated that rice husk–orange peel constituents remained associated with the nanoparticle surface, which is consistent with a capping/stabilizing role and with FTIR features reported for phytochemically synthesized iron oxide nanoparticles [6].

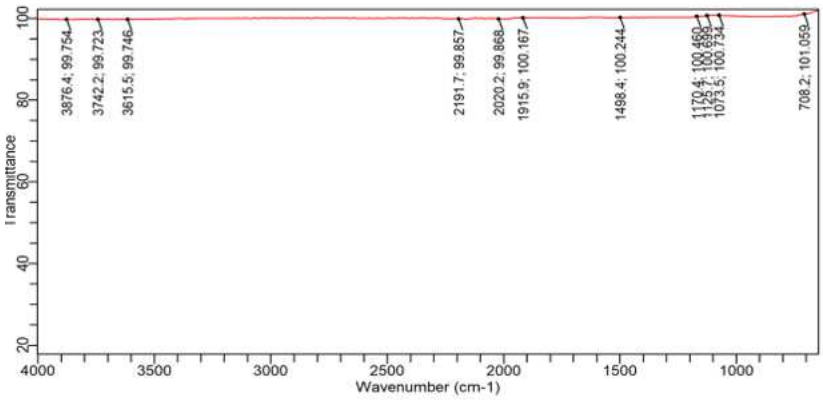

Figure 2. FTIR spectrum of RHOPTNPs

3.1.3. DLS Analysis

Dynamic light scattering (DLS) analysis, shown in Fig. 3 and Fig. 4 revealed that RHOPTNPs possessed an average hydrodynamic diameter of 76.24 nm with a polydispersity index (PDI) of 0.411, indicative of a moderately polydisperse population. This size distribution is comparable to other green-synthesized iron oxide nanomaterials prepared from agricultural biomass extracts [3, 12]. The incorporation of the residual biomass template, together with the combined rice husk–orange peel extract, likely influenced nanoparticle nucleation and growth, resulting in slightly larger hydrodynamic dimensions. The observed increase in size may also be attributed to surface-bound phytochemicals and hydrated organic layers associated with the biomass template, which contribute to particle stabilization and steric hindrance in aqueous suspension [4, 6]. Similar effects have been reported in other phytochemical-mediated syntheses, where organic capping layers increase the apparent hydrodynamic diameter relative to crystallite sizes determined by XRD or SEM [7, 13].

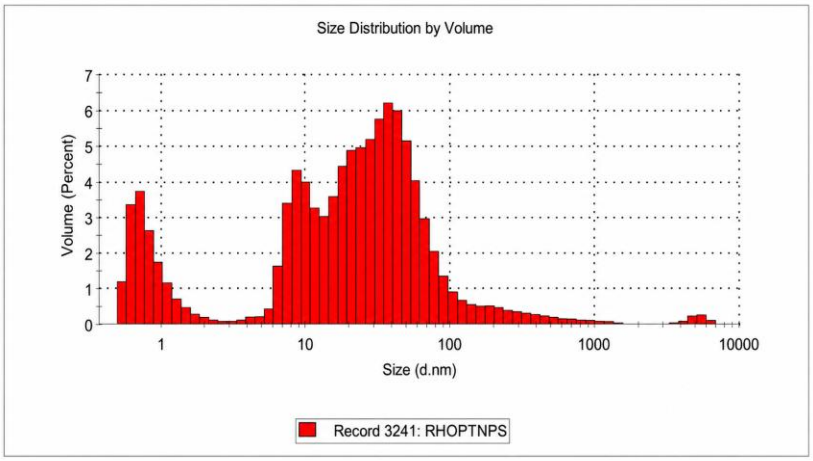

Figure 3. Particle size distribution of RHOPTNPs by Volume

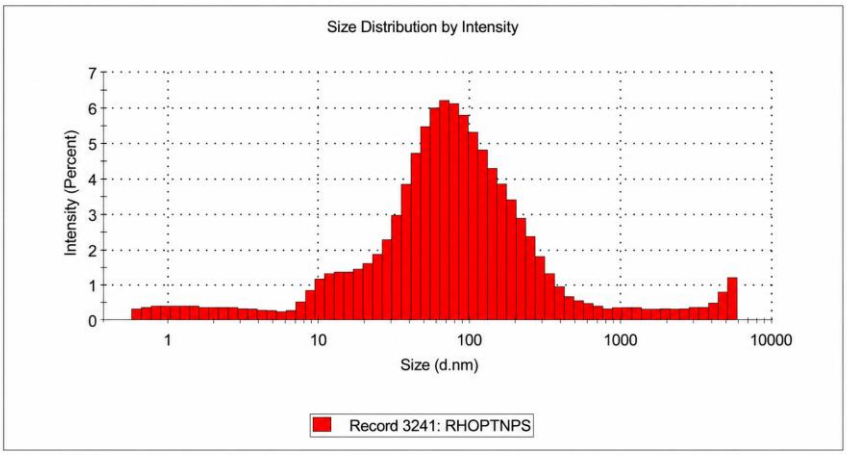

Figure 4. Particle size distribution of RHOPTNPs by intensity

3.1.4. SEM–EDS Analysis

SEM micrographs of RHOPTNPs (Fig. 5), obtained at magnifications of 8000–10,000×, revealed an irregular and agglomerated morphology. The observed aggregation is consistent with the tendency of nanoscale metal oxide particles to undergo interparticle interactions, particularly in the presence of surface-bound biomolecules derived from plant materials.

The EDS spectrum (Fig. 6) confirmed Fe, O and C as the major elemental constituents (77.85, 20.02 and 3.22 wt%, respectively), consistent with an iron oxide phase bearing residual organic matter from the rice husk–orange peel extract and residue on the nanoparticle surface.

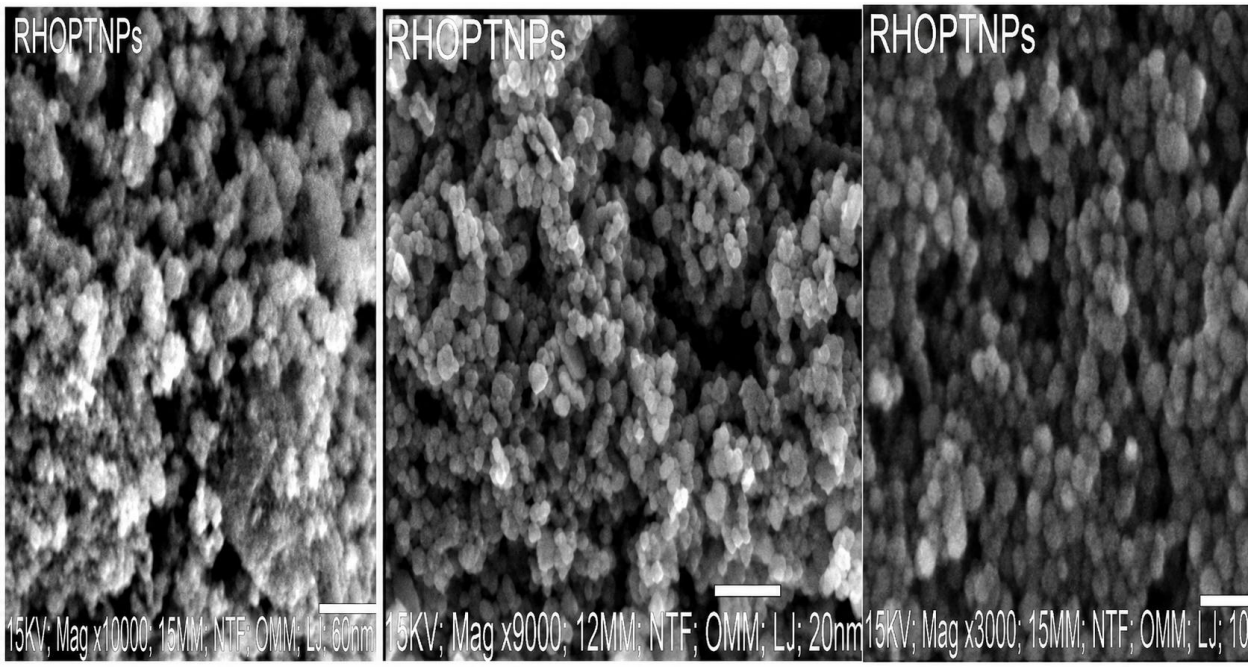

Figure 5. SEM micrographs of RHOPTNPs at magnifications of 10 000×, 9000× and 8000×

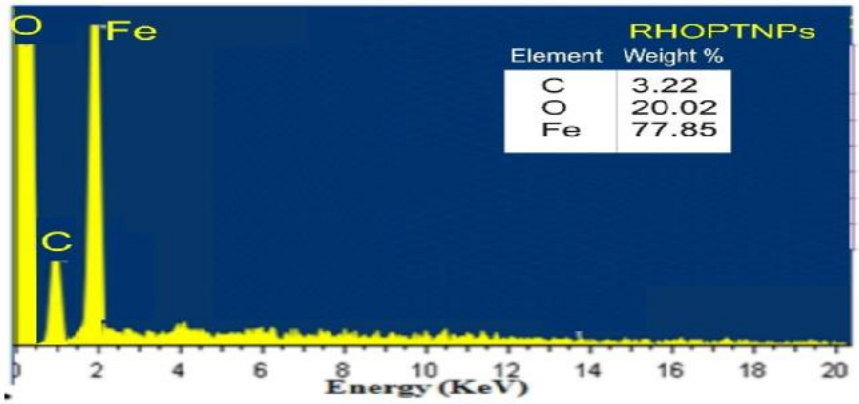

Figure 6. EDS spectrum of RHOPTNPs

3.1.5. XRD Analysis

The XRD pattern of RHOPTNPs (Fig. 7) exhibited characteristic diffraction peaks at 2θ = 30.25° (220), 35.64° (311), 57.33° (511), and 62.96° (440), consistent with the characteristic reflections

of magnetite (Fe_3O_4). The observed reflections showed good agreement with PDF/JCPDS No. 01-075-0449, confirming the formation of a cubic spinel structure with space group $Fd\bar{3}m$ (No. 227). Because magnetite (Fe_3O_4) and maghemite (γ-Fe_2O_3) share closely related cubic spinel structures and nearly indistinguishable XRD reflections, this pattern is best described as a magnetite-consistent cubic iron oxide phase, as XRD alone cannot conclusively rule out a maghemite or mixed-phase composition. The mean crystallite size, calculated using the Debye–Scherrer equation from the most intense (311) reflection at $2\theta = 35.64°$, was 77.16 nm. This value was comparable to the DLS-derived Z-average hydrodynamic diameter of 76.24 nm, but larger than the 20–35 nm particle dimensions observed by SEM. The differences reflect the distinct length scales measured by the three techniques: XRD estimates coherent crystalline domains, DLS measures the hydrated hydrodynamic diameter of dispersed particles, and SEM provides the physical dimensions of individual particles. The relatively high PDI (0.411) further indicates particle-size heterogeneity, which may contribute to the differences among the measured dimensions. The sharp and intense diffraction peaks indicate good crystallinity of the magnetite-consistent iron oxide phase, whereas the less-defined background features may be associated with amorphous biomass-derived components retained on the nanoparticle surface. In conjunction with the surface functional groups identified by FTIR, the crystalline and surface characteristics of RHOPTNPs provide structural features that may contribute to their interaction with and adsorption of pharmaceutical contaminants [14-17].

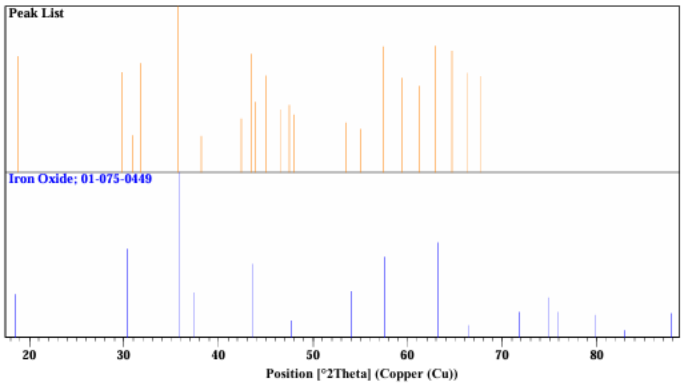

Figure 7. XRD diffractograph of RHOPTNPs matched against reference pattern (Iron Oxide; 01-075-0449)

3.1.6. BET Surface Area and Porosity Analysis

The BET analysis showed that RHOPTNPs exhibited a specific surface area of 846.28 $m^2\ g^{-1}$, indicating a highly developed surface suitable for adsorption. The Langmuir surface area was estimated at 160.54 $m^2\ g^{-1}$, further demonstrating the availability of adsorption sites on the RHOPTNPs surface.

RHOPTNPs also recorded the highest total pore volume (0.658 $cm^3\ g^{-1}$), suggesting a well-developed porous structure that may facilitate the diffusion and retention of pharmaceutical molecules. The adsorption–desorption isotherm (Fig. 8) was classified as Type II, with adsorption occurring over a relative pressure range of approximately 0.05–0.85 (P/P_0) and approaching saturation at $P/P_0 \approx 0.90$. This profile indicates multilayer adsorption on a surface with limited microporosity and/or macroporous characteristics

Together with the surface functional groups identified by FTIR, this high surface area, Langmuir surface area and pore volume indicate favourable textural characteristics for adsorbing ciprofloxacin and ibuprofen from aqueous media.

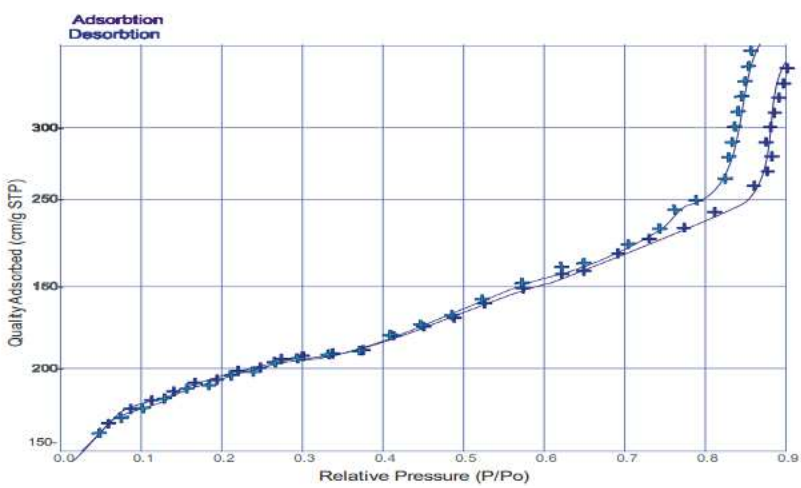

Figure 8. N_2 adsorption-desorption isotherm (BET) of RHOPTNPs

Table 1. BET surface area and porosity data for RHOPTNPs

Nanoparticle	BET surface area ($m^2 g^{-1}$)	Langmuir surface area ($m^2 g^{-1}$)	Pore volume ($cm^3 g^{-1}$)	Isotherm type	Condensation range
RHOPTNPs	846.28	160.54	0.6582	Type II	0.05–0.85

3.1.7. Thermogravimetric Analysis

The TGA profile of RHOPTNPs (Fig. 9) showed an initial weight loss of approximately 0.30% between 0 and 98 °C, attributable to the removal of physically adsorbed moisture. A pronounced mass loss of 29.50% occurred between 250 and 330 °C, which can be associated with the thermal degradation of biomass-derived organic constituents, including hydroxyl-containing compounds, polyphenols, and other phytochemicals retained from the rice husk–orange peel extract and residue template.

Above approximately 330 °C, no substantial further mass loss occurred up to 600 °C, confirming good thermal stability of the remaining inorganic phase. Together, these results indicate that RHOPTNPs comprise a thermally stable magnetite core carrying a substantial fraction of surface-bound biomass-derived organic matter, which may contribute additional functional groups relevant to pharmaceutical adsorption.

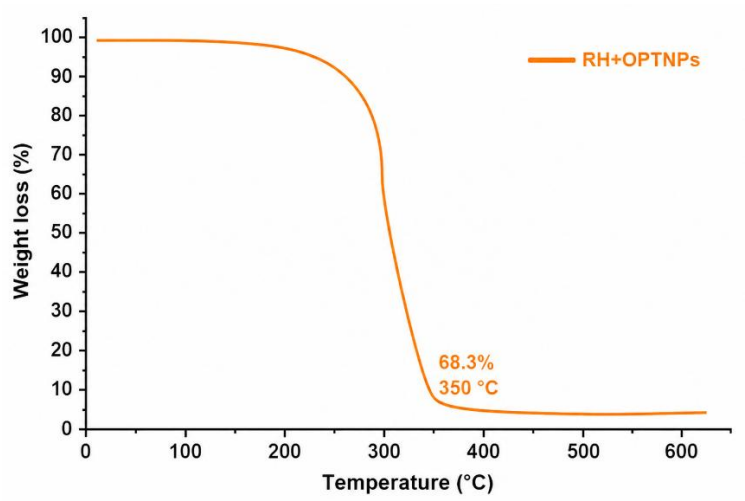

Figure 9. TGA curves of the synthesized iron oxide nanoparticles, including RHOPTNPs

3.2 Result of Batch Adsorption for the Removal of Ciprofloxacin and Ibuprofen from water

3.2.1 Effect of Adsorbent Dose and Contact Time on Pharmaceutical Removal by RHOPTNPs

The effects of adsorbent dose and contact time on the removal of ciprofloxacin and ibuprofen by RHOPTNPs were systematically evaluated under identical experimental conditions (initial concentration 6 mg L^{-1}, pH 7.0, 27 °C, agitation speed 200 rpm) (Fig. 10).

Ciprofloxacin removal efficiency increased progressively with both adsorbent dose and contact time, reaching a maximum of 88.93% at a dose of 80 mg and a contact time of 40 min. The enhancement in removal with increasing dosage can be attributed to the greater number of active adsorption sites and the correspondingly larger surface area available for interaction, while the time-dependent increase reflects progressive interaction between ciprofloxacin molecules and the RHOPTNP surface as the system approached equilibrium. Beyond 80 mg, no substantial further improvement was observed, suggesting that this dosage already provided sufficient accessible binding sites to accommodate the ciprofloxacin present in solution, consistent with trends reported elsewhere for biomass-derived adsorbents [18, 19].

A similar trend was observed for ibuprofen, with removal efficiency increasing with both dose and contact time to a maximum of 92.21% at 60 mg and 35 min. As with ciprofloxacin, the improvement with increasing dosage is consistent with greater adsorption site availability; however, the absence of proportional gains beyond 60 mg is likely attributable to particle aggregation and the resultant overlap of active sites at higher adsorbent loadings, which effectively reduces the surface area accessible per unit mass [20]. The observed time-dependent behaviour is consistent with progressive diffusion of ibuprofen molecules into the pore structure of RHOPTNPs, with equilibrium attained at approximately 35 min. Comparable contact-time-dependent adsorption behaviour for ibuprofen has previously been reported for magnetic and carbon-based nanomaterials [21, 22].

The comparatively high removal efficiencies obtained for both pharmaceuticals are consistent with the favourable surface properties of RHOPTNPs, including their high pore volume and the biomass-derived functional groups identified through BET and FTIR analyses. These characteristics enhance the accessibility of adsorption sites and promote strong adsorbate–adsorbent interactions, thereby supporting efficient contaminant uptake.

The optimum removal conditions were an 80 mg adsorbent dose and 40 min contact time, which gave 88.93% ciprofloxacin removal, and a 60 mg adsorbent dose and 35 min contact time, which gave 92.21% ibuprofen removal. These findings underscore the potential of RHOPTNPs as an effective, waste-derived nanomaterial for the removal of pharmaceutical contaminants from aqueous systems.

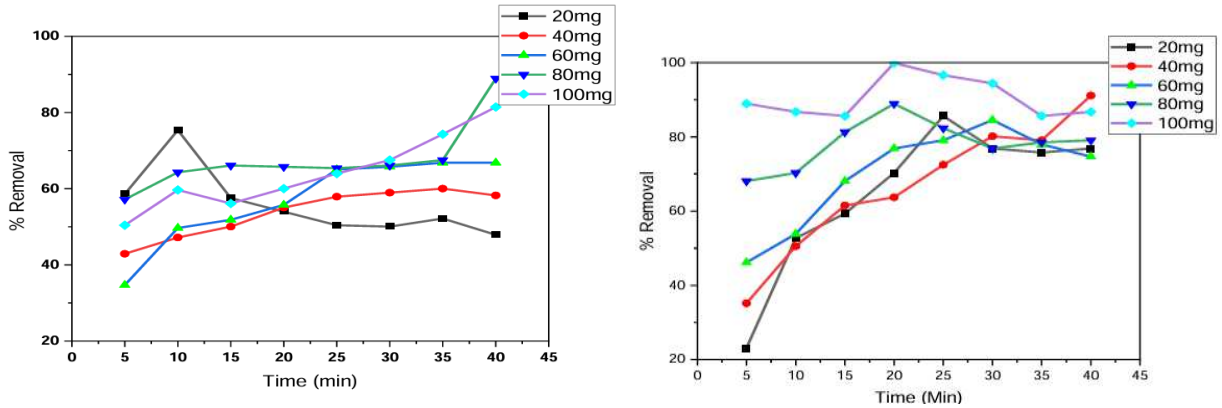

Figure 10. Effect of adsorbent dosage and shaking time on the removal of ciprofloxacin and ibuprofen

3.2.2 Effect of Solution pH and Point of Zero Charge on Pharmaceutical Adsorption

The point of zero charge (pHpzc) of RHOPTNPs was determined to be 7.0 ± 0.1 (Fig. 11), indicating that the nanoparticle surface is positively charged below this pH and negatively charged above it, consistent with the salt-addition method [9].For ciproflox

acin, the optimum adsorption was observed at pH 7 (Fig. 12), coinciding with the pHpzc and yielding approximately 75% removal efficiency. At this pH, ciprofloxacin exists predominantly in its zwitterionic form, enabling electrostatic attraction to be complemented by hydrogen bonding and π–π interactions with aromatic and phenolic moieties on the RHOPTNP surface. Removal

efficiency declined at higher pH values, reflecting reduced electrostatic affinity as the surface became increasingly negative.

For ibuprofen, adsorption efficiency was strongly pH-dependent, increasing from acidic conditions and reaching a maximum of 74% at pH 9. Ibuprofen, with a pKa of 5.2, exists mainly in its anionic form above this pH. Since RHOPTNPs are negatively charged above pHpzc, the relatively high removal observed at pH 7–9 suggests that electrostatic interactions alone do not govern adsorption. Instead, additional mechanisms such as hydrogen bonding, surface complexation, and hydrophobic interactions involving biomass-derived functional groups likely contribute to uptake. Similar pH-dependent behaviour has been reported for ibuprofen adsorption using magnetic and carbon-based adsorbents [23-25].

The results demonstrate that solution pH is a critical parameter controlling adsorption performance. Ciprofloxacin removal was maximized at neutral pH (7.0), coinciding with the pHpzc, while ibuprofen removal was favoured under slightly alkaline conditions (pH 9). These findings highlight the importance of tailoring adsorption conditions to the physicochemical properties of both the adsorbent and the pharmaceutical contaminant.

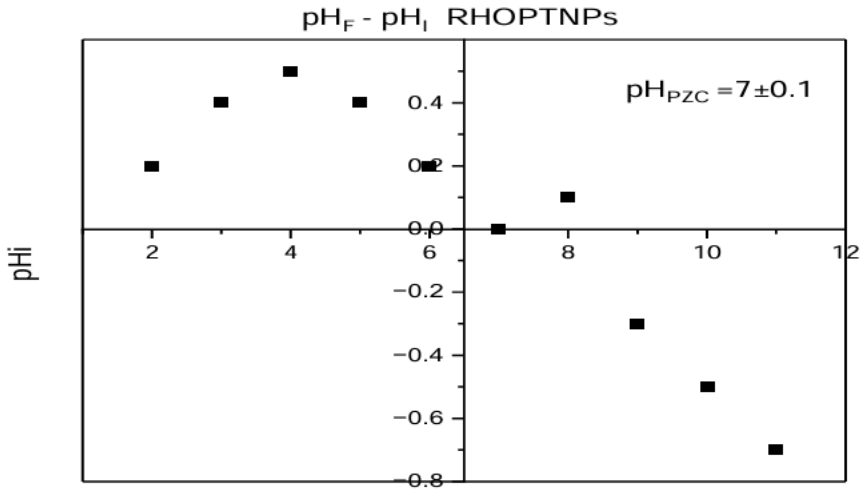

Figure 11. Point of zero charge (pHpzc) of RHOPTNPs

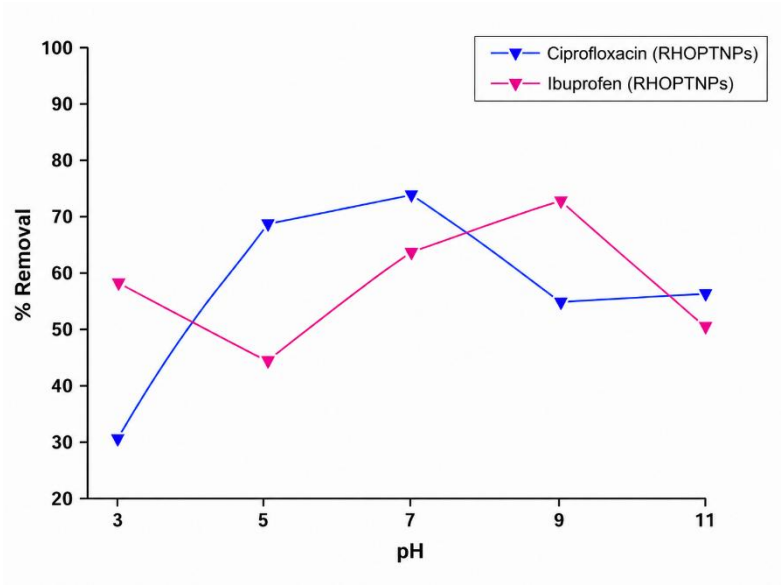

Figure 12. Effect of solution pH on the adsorption of ciprofloxacin and ibuprofen

3.2.3 Effect of Initial Adsorbate Concentration

The influence of initial adsorbate concentration on the adsorption of ciprofloxacin and ibuprofen by RHOPTNPs was examined over the range of 2–10 mg L^{-1} under optimized conditions (Fig. 13).

For ciprofloxacin, experiments conducted with 80 mg RHOPTNPs, 40 min contact time, pH 7.0, and room temperature showed removal efficiency increasing steadily with concentration, reaching a maximum of 94.86% at 10 mg L^{-1}. This corresponds to a Langmuir adsorption capacity () of 9.34 mg g^{-1}, which is lower than the 51.2 mg g^{-1} reported for rice husk-derived IONPs [26] and 27.8 mg g^{-1} for orange peel-derived IONPs [27]. Although the capacity is modest, RHOPTNPs achieved high removal efficiency at environmentally relevant concentrations, underscoring their practical applicability. The enhanced uptake is attributed to the concentration gradient between the aqueous phase and the RHOPTNP surface, which promotes mass transfer and diffusion of ciprofloxacin molecules to available adsorption sites [28].For ibuprofen

, adsorption was evaluated using 60 mg RHOPTNPs and 35 min contact time. Removal efficiency remained relatively stable across the tested concentration range, with a Langmuir of 112.36 mg g^{-1}. This value is substantially higher than the 35.4 mg g^{-1} reported for Fe_3O_4-activated carbon composites [29] and 42.7 mg g^{-1} for magnetized biochar [30], highlighting the superior adsorption capacity of RHOPTNPs for ibuprofen. The stable performance suggests that sufficient active sites

were available relative to the ibuprofen concentration, ensuring consistent uptake. At higher concentrations, competition among ibuprofen molecules for adsorption sites may become more pronounced, potentially leading to surface saturation and reduced efficiency [31].Collectivey,R

HOPTNPs demonstrated high adsorption efficiency for ciprofloxacin at low concentrations and exceptional capacity for ibuprofen, outperforming several benchmark adsorbents. These quantitative comparisons emphasize both the strengths and limitations of RHOPTNPs, confirming their suitability as a sustainable nanomaterial for pharmaceutical contaminant removal.

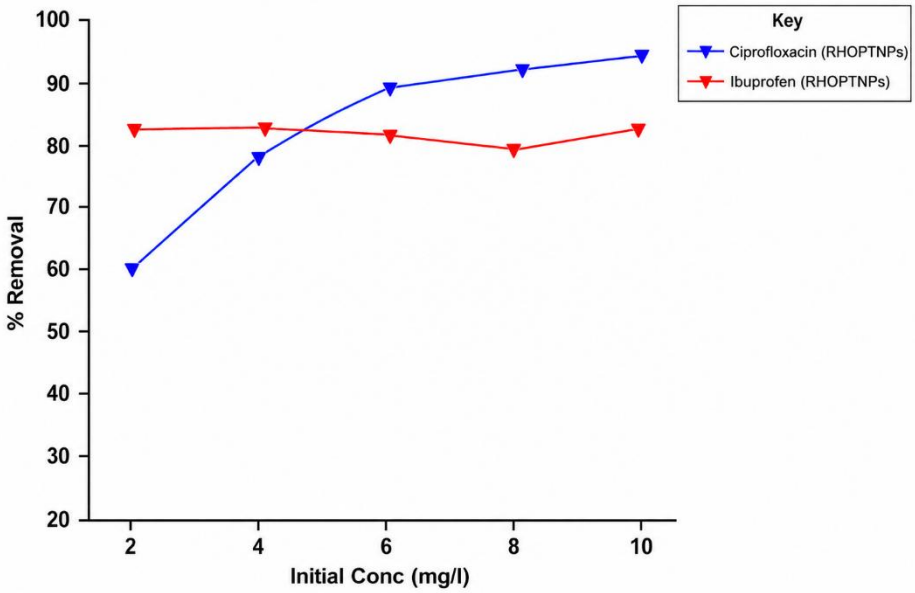

Figure 13. Effect of initial adsorbate concentration on the removal of ciprofloxacin ibuprofen

3.2.4 Effect of Temperature on Ciprofloxacin and Ibuprofen Adsorption

The effect of temperature on the adsorption of ciprofloxacin and ibuprofen by RHOPTNPs was investigated over the range of 300–320 K under the respective optimized experimental conditions (Fig. 14). Ciprofloxacin removal increased progressively with increasing temperature, reaching a maximum removal efficiency of 99.45% at 320 K. The enhanced adsorption at elevated temperatures suggests that the process is thermally favoured and may exhibit an endothermic character. Increased temperature can enhance the mobility and diffusion of ciprofloxacin molecules in solution, thereby facilitating mass transfer and interaction with available adsorption sites on RHOPTNPs [32, 33]. In addition, the removal of weakly bound water molecules from the

adsorbent surface at higher temperatures may improve the accessibility of active sites. Similar temperature-dependent increases in ciprofloxacin adsorption have been reported for iron oxide-based and other nanoparticle adsorbents [18, 34].

In contrast, ibuprofen adsorption decreased with increasing temperature, declining from approximately 80.15% at 300 K to 53.83% at 320 K (Fig. 14). This trend indicates that ibuprofen adsorption onto RHOPTNPs is favoured at lower temperatures and is consistent with an exothermic adsorption process. At elevated temperatures, increased molecular mobility may weaken adsorbate–adsorbent interactions and promote desorption, thereby reducing the net absorption of ibuprofen. Similar temperature-dependent reductions in ibuprofen adsorption have been reported for other adsorbent systems [35, 36]. The contrasting behaviour observed for ciprofloxacin and ibuprofen may be attributed to differences in their physicochemical properties and interactions with the surface functional groups of RHOPTNPs.

Generally, temperature exerted a significant but contrasting influence on the adsorption of the two pharmaceuticals. Higher temperatures enhanced ciprofloxacin removal, with optimum performance observed at 320 K, whereas ibuprofen adsorption was favoured at 300 K. These findings demonstrate that the adsorption behaviour of RHOPTNPs is strongly dependent on the nature of the adsorbate and its interaction with the nanoparticle surface.

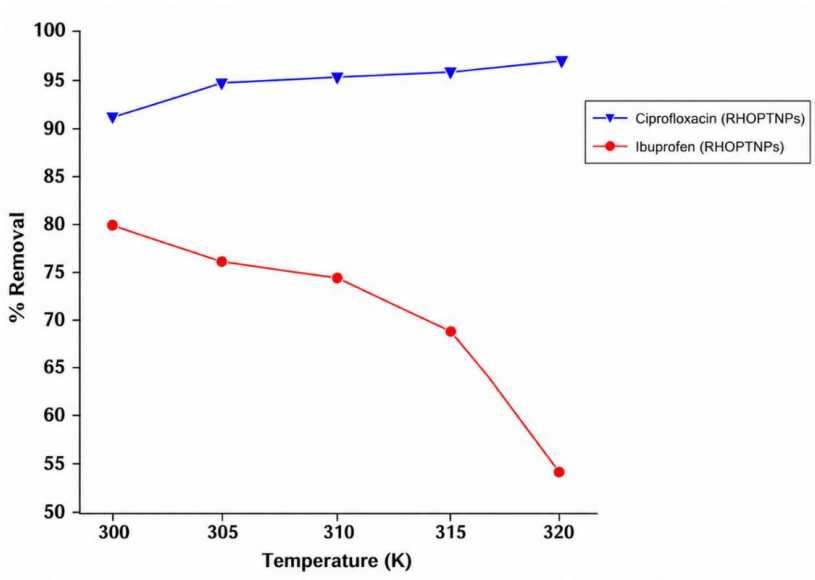

Figure 14. Effect of temperature on the adsorption of ciprofloxacin and ibuprofen

3.2.5 Thermodynamic Studies of Ciprofloxacin and Ibuprofen Adsorption by RHOPTNPs

The thermodynamic parameters for the adsorption of ciprofloxacin and ibuprofen onto RHOPTNPs are presented in Table 2. The two pharmaceuticals exhibited distinct thermodynamic behaviours. For ciprofloxacin, the negative ΔG values obtained across the investigated temperature range indicate that adsorption was spontaneous and thermodynamically favourable. The increasing magnitude of ΔG with temperature, together with the positive ΔH value (87.95 kJ/mol), indicates that ciprofloxacin adsorption was enhanced at elevated temperatures and was therefore endothermic. The positive ΔS value (313.88 J/mol K) suggests increased randomness at the solid–liquid interface, possibly associated with the release of previously adsorbed water molecules and molecular rearrangement during adsorption. The relatively high ΔH value further suggests the contribution of strong adsorbate–adsorbent interactions. Similar spontaneous and endothermic behaviour has been reported for ciprofloxacin adsorption using iron-based and magnetic adsorbents [18, 37, 38].

In contrast, ibuprofen adsorption onto RHOPTNPs exhibited negative ΔG values but a negative ΔH value (−38.49 kJ/mol), indicating a spontaneous and exothermic process. The decrease in the magnitude of ΔG with increasing temperature suggests that adsorption became less favourable at elevated temperatures, consistent with the decrease in ibuprofen removal observed in the temperature study. The negative ΔS value (−109.08 J/mol K) indicates a decrease in interfacial randomness, which may result from the formation of relatively ordered ibuprofen–RHOPTNP surface complexes. The thermodynamic behaviour suggests that ibuprofen adsorption is governed by a combination of surface interactions, including electrostatic attraction, hydrogen bonding and other specific interactions.

Generally, the contrasting thermodynamic profiles demonstrate the adsorbate-dependent nature of RHOPTNPs. Ciprofloxacin adsorption was spontaneous and endothermic, whereas ibuprofen adsorption was spontaneous and exothermic. These differences can be attributed to the distinct molecular structures, ionization characteristics and interactions of the two pharmaceuticals with the functionalized iron oxide surface. The results further confirm the suitability of RHOPTNPs for the adsorption-based removal of both pharmaceuticals from aqueous media.

Table 2. Thermodynamic Parameters for the Adsorption of Ciprofloxacin and Ibuprofen

Adsorbent	Pollutant	Temperature (K)	ΔG (kJ mol⁻¹)	ΔH (kJ mol⁻¹)	ΔS (J mol⁻¹ K⁻¹)
RHOPTNPs	Ciprofloxacin	300	−6.21	87.85	313.88
		305	−7.78		
		310	−9.35		
		315	−10.92		
		320	−12.49		
RHOPTNPs	Ibuprofen	300	−5.76	−38.49	−109.08
		305	−5.22		
		310	−4.67		
		315	−4.13		
		320	−3.58		

3.3 Reusability of RHOPTNPs for Ciprofloxacin and Ibuprofen Removal

The reusability of RHOPTNPs was evaluated through four successive adsorption–desorption cycles for the removal of ciprofloxacin and ibuprofen. RHOPTNPs demonstrated good regeneration performance for ciprofloxacin, with the removal efficiency decreasing from 82.16% in the first cycle to 75.90% in the fourth cycle, representing an absolute reduction of 6.26 percentage points, or approximately 7.62% relative to the initial removal efficiency. For ibuprofen, the removal efficiency decreased from 97.45% in the first cycle to 64.44% in the fourth cycle, corresponding to an absolute reduction of 33.01 percentage points and a relative decline of approximately 33.87%. The more pronounced decline observed for ibuprofen suggests greater loss of adsorption performance during repeated regeneration compared with ciprofloxacin. This reduction may be associated with incomplete desorption of the adsorbed pharmaceuticals, residual

molecules occupying active adsorption sites, and possible alteration or loss of accessible surface sites during successive adsorption–desorption cycles [18].The relativel

y small reduction in ciprofloxacin removal indicates that RHOPTNPs retain a substantial proportion of their adsorption performance after repeated regeneration. In contrast, the larger decline observed for ibuprofen indicates a greater reduction in adsorption capacity over successive cycles. Nevertheless, the adsorbent retained 92.38% of its initial ciprofloxacin removal efficiency and 66.13% of its initial ibuprofen removal efficiency after the fourth cycle. In addition, the magnetic nature of RHOPTNPs facilitates their rapid separation and recovery from treated water, which is advantageous for repeated batch adsorption operations. The observed reusability is consistent with the potential of magnetic iron-based adsorbents and nanocomposites for repeated pharmaceutical removal applications [18, 39].

The results generally demonstrate that RHOPTNPs can be regenerated and reused over multiple adsorption cycles, although their regeneration stability is substantially higher for ciprofloxacin than for ibuprofen. After four cycles, RHOPTNPs retained approximately 92.38% and 66.13% of their initial removal efficiencies for ciprofloxacin and ibuprofen, respectively. Thus, while the adsorbent exhibits good recyclability for ciprofloxacin, the pronounced decline in ibuprofen removal suggests that further optimization of the regeneration procedure may be necessary to maintain its adsorption performance during repeated use. The combination of reusability and magnetic recoverability nevertheless supports the potential application of RHOPTNPs as a recoverable adsorbent for pharmaceutical-contaminated water.

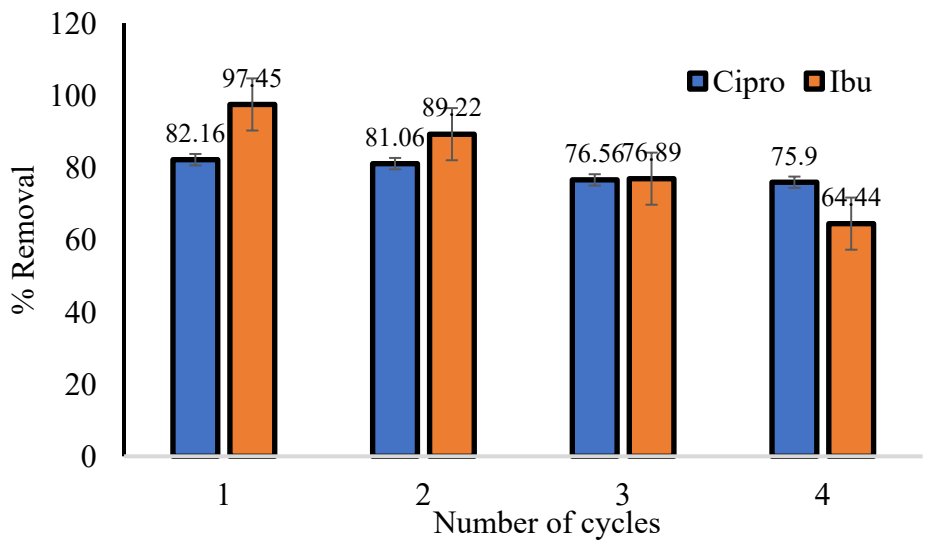

Figure 15: Result of the reusability of the synthesized Adsorbent

3.4 Adsorption Isotherms of Ciprofloxacin and Ibuprofen on RHOPTNPs

The equilibrium adsorption of ciprofloxacin and ibuprofen onto RHOPTNPs was evaluated using the Langmuir, Freundlich and Temkin isotherm models (Table 3). For ciprofloxacin, the Langmuir model gave the highest correlation coefficient (R_2=0.9179), compared with 0.8896 for both the Freundlich and Temkin models, indicating that the Langmuir model provided the best description of the equilibrium data. The calculated maximum adsorption capacity (q_m) was 9.34 mg g^{-1}, with a Langmuir affinity constant (K_L) of 0.689 L mg^{-1}. The separation factor (R_L=0.0193) was within the favourable range of ($0<R_L<1$), confirming favourable adsorption of ciprofloxacin onto RHOPTNPs, consistent with previous reports of favourable pharmaceutical adsorption using iron-based and biomass-derived adsorbents [18, 40].

For ibuprofen, the Langmuir model exhibited an excellent fit (R^2=0.9929), higher than those obtained for the Freundlich (R^2=0.9678) and Temkin (R^2=0.9678) models. The Langmuir maximum adsorption capacity was 112.36 mg g^{-1}, with (K_L=0.0561) L mg^{-1} and (R_L=0.0561), confirming favourable adsorption. The relatively high (q_m) demonstrates the substantial adsorption capacity of RHOPTNPs towards ibuprofen. This value compares favourably with adsorption capacities reported for several iron-based and nanostructured adsorbents, indicating the effectiveness of RHOPTNPs for ibuprofen removal [21, 29, 41].

The Freundlich model also indicated favourable adsorption of ibuprofen, with (n=1.05) and (R^2=0.9678), while the Temkin model showed a similarly strong correlation ((R^2=0.9678)). However, the higher (R^2) obtained for the Langmuir model suggests that monolayer adsorption on relatively homogeneous active sites provides the most appropriate representation of the equilibrium behaviour. The good Temkin fit further suggests that adsorbate–adsorbent interactions and variations in adsorption energy may also contribute to the process [42].

The isotherm analysis demonstrates that RHOPTNPs exhibit favourable adsorption towards both ciprofloxacin and ibuprofen, with the equilibrium data better described by the Langmuir model. The substantially higher adsorption capacity observed for ibuprofen may be associated with the surface characteristics of RHOPTNPs, including their surface functional groups, pore structure and biomass-derived surface components. Similar influences of surface area, particle characteristics and functional groups on pharmaceutical adsorption have been reported previously ([43, 44]). The low (R_L) values further confirm the favourable nature of the adsorption process and support the potential application of RHOPTNPs for the removal of pharmaceutical contaminants from aqueous media.

Table 3. Adsorption isotherm parameters for ciprofloxacin and ibuprofen adsorption

Isotherm Model	Parameter	Ciprofloxacin	Ibuprofen
Langmuir	(mg g^{-1})	9.337	112.360
	(L mg^{-1})	0.689	0.056
		0.019	0.056
		0.918	0.993
Freundlich		2.207	0.951
		0.453	1.051
	(mg g^{-1} (L mg^{-1})$^{1/n}$)	2.777	5.936

Isotherm Model	Parameter	Ciprofloxacin	Ibuprofen
		0.890	0.968
Temkin		0.864	0.951
		1.434	1.781
	($L\ g^{-1}$)	4.201	5.936
	($L\ mol^{-1}$)	2868.5	2673.2
		0.890	0.968

3.5 Kinetic Studies of Ciprofloxacin and Ibuprofen Adsorption Using RHOPTNPs

The adsorption kinetics of ciprofloxacin and ibuprofen onto RHOPTNPs were evaluated using pseudo-first-order, pseudo-second-order, intraparticle diffusion, and Elovich models (Table 4). For ciprofloxacin, the pseudo-first-order model showed a poor fit, with an (R_2) value of 0.44193 and a negative (k_1) value (−0.00030 min^{-1}), indicating that this model inadequately describes the adsorption process. In contrast, the pseudo-second-order model provided a better fit (R^2=0.91244), with an equilibrium adsorption capacity (q_e) of 3.08 mg/g and (k_2) of 0.08120 g/mg min. This suggests that the adsorption rate is predominantly associated with interactions between the adsorbate and active sites on RHOPTNPs [31, 45].

The intraparticle diffusion model gave a relatively poor fit for ciprofloxacin (R^2=0.44422), suggesting that intraparticle diffusion alone was not the controlling rate-limiting mechanism. The Elovich model also showed a weak fit (R^2=0.37838), although its parameters indicate the presence of heterogeneous adsorption sites. Overall, the kinetic behaviour of ciprofloxacin on RHOPTNPs is best represented by the pseudo-second-order model, indicating a predominantly chemisorption-controlled process.

For ibuprofen, the pseudo-second-order model also provided the best kinetic description, with (R^2=0.98642), (q_e=3.58) mg/g and (k_2=0.06592) g/mg min. The relatively high (R^2) and positive (k_2) value indicate strong agreement between the experimental data and the pseudo-second-order model. The pseudo-first-order model gave a lower (R^2) of 0.66676, while the intraparticle diffusion and Elovich models produced (R^2) values of 0.77727 and 0.84607, respectively. These results indicate that although diffusion and surface heterogeneity contribute to the adsorption process, they do not adequately describe the overall adsorption kinetics.

The pseudo-second-order model therefore best describes the adsorption of both ciprofloxacin and ibuprofen onto RHOPTNPs. The results suggest that surface interactions between the pharmaceutical molecules and the active sites of RHOPTNPs play a major role in controlling the adsorption rate, consistent with the chemisorption mechanism proposed for heterogeneous adsorbent surfaces [46, 47].

Table 4. Kinetic model parameters for the adsorption of ciprofloxacin and ibuprofen

Kinetic Model	Parameter	Ciprofloxacin	Ibuprofen
Pseudo-First-Order	(mg g^{-1})	2.598	5.402
	(min^{-1})	−0.00030	−0.00018
		0.442	0.667
Pseudo-Second-Order	(mg g^{-1})	3.083	3.581
		9.503	12.823
	(g mg^{-1} min^{-1})	0.081	0.057
		0.912	0.986

Kinetic Model	Parameter	Ciprofloxacin	Ibuprofen
Intraparticle Diffusion	(mg g^{-1} $min^{1/2}$)	0.177	0.313
	(mg g^{-1})	1.371	1.430
		0.444	0.777
Elovich	(mg g^{-1} min^{-1})	68.436	2.833
	(g mg^{-1})	2.995	1.835
		0.378	0.864

3.6 Application to Real Wastewater

The occurrence of ciprofloxacin and ibuprofen in selected hospital and domestic wastewater samples from Kaduna metropolis was investigated, followed by adsorption treatment using RHOPTNPs. The results are presented in Tables 5 and 6.

In hospital wastewater, ciprofloxacin concentrations ranged from 1.31 to 1.89 mg L^{-1}. Treatment with RHOPTNPs resulted in removal efficiencies of 80.95%, 82.44%, and 84.09% for BDTH, YSDH, and PHCBR, respectively, demonstrating effective removal of ciprofloxacin from complex hospital wastewater matrices. The slightly lower removal efficiencies compared with controlled batch experiments may be associated with the presence of competing dissolved organic and inorganic constituents in real wastewater, which can occupy or interfere with available adsorption sites. Similar applications of iron-based nanomaterials for ciprofloxacin-contaminated wastewater have demonstrated the potential of adsorption-based processes, particularly when combined with oxidative treatment mechanisms [48-50].

Ibuprofen concentrations in hospital wastewater ranged from 0.78 to 1.44 mg L^{-1}. RHOPTNPs achieved high removal efficiencies of 86.80%, 96.15%, and 96.19% for BDTH, YSDH, and

PHCBR, respectively. The consistently high removal of ibuprofen suggests favourable interactions between ibuprofen molecules and the active surface sites of RHOPTNPs. The adsorption behaviour may be influenced by electrostatic interactions, hydrogen bonding, and other surface interactions associated with the iron oxide surface and biomass-derived functional groups [51]. These results support the potential application of plant-mediated iron oxide nanoparticles for pharmaceutical removal from hospital wastewater, although issues relating to nanoparticle stability, regeneration, and post-treatment management require further consideration [51-53].

In domestic wastewater, ciprofloxacin concentrations ranged from 0.91 to 1.51 mg L^{-1} across the sampled locations. RHOPTNPs achieved removal efficiencies of 94.50%, 86.09%, and 84.31% for Samples A, B, and C, respectively. Similarly, ibuprofen concentrations ranged from 0.68 to 1.30 mg L^{-1}, with removal efficiencies of 97.05%, 93.07%, and 93.85%, respectively. The results demonstrate that RHOPTNPs maintained substantial adsorption performance in real domestic wastewater, with ibuprofen generally showing higher removal than ciprofloxacin.

The detected pharmaceutical concentrations differed from values reported for urban wastewater in other regions, which may reflect differences in pharmaceutical consumption, wastewater sources, disposal practices, and treatment infrastructure [54]. The occurrence of ciprofloxacin and ibuprofen in untreated wastewater is environmentally significant because of their persistence and potential ecological effects, including the contribution of antibiotic residues to antimicrobial resistance [54-56]. Consequently, the high removal efficiencies obtained in this study indicate that RHOPTNPs have potential as a low-cost, biomass-derived adsorbent for reducing pharmaceutical residues in hospital and domestic wastewater.

Table 5. Occurrence of ciprofloxacin and ibuprofen in hospital wastewater and their removal by RHOPTNPs

Sn	Sample	Initial CIP Conc. (mg/L)	CIP Removal (%)	Initial IBU Conc. (mg/L)	IBU Removal (%)
1	BDTH	1.89	80.95	1.44	86.80
2	YSDH	1.31	82.44	0.78	96.15
3	PHCBR	1.32	84.09	1.05	96.19

Table 6. Occurrence of ciprofloxacin and ibuprofen in domestic wastewater and their removal by RHOPTNPs

Sn	Sample	Initial CIP Conc. (mg/L)	CIP Removal (%)	Initial IBU Conc. (mg/L)	IBU Removal (%)
1	A	0.91	94.50	0.68	97.05
2	B	1.51	86.09	1.30	93.07
3	C	1.02	84.31	1.14	93.85

4.0 Conclusion

Iron oxide nanoparticles were successfully green-synthesized using a combined rice husk-orange peel extract and residue template (RHOPTNPs) and characterized by UV-Vis, FTIR, DLS, SEM-EDS, XRD, BET, and TGA analyses, confirming the formation of a phytochemically capped, cubic iron oxide nanostructure with an average particle size of 76.24 nm and a high BET surface area of 846.28 m^2/g. RHOPTNPs demonstrated strong performance as an adsorbent for the removal of ciprofloxacin (up to 99.45% removal) and ibuprofen (up to 84% removal) from aqueous solution under optimized batch conditions. Adsorption of both pharmaceuticals was best described by the Langmuir isotherm and pseudo-second-order kinetics, indicating chemisorption-dominated, monolayer uptake; ciprofloxacin adsorption was spontaneous and endothermic, while ibuprofen adsorption was spontaneous and exothermic. RHOPTNPs retained good removal performance across repeated adsorption cycles and effectively removed both pharmaceuticals from real hospital and domestic wastewater. These findings support RHOPTNPs, derived from low-cost, readily

available agrowaste, as a promising, sustainable, and reusable adsorbent for the remediation of pharmaceutically contaminated water, warranting further investigation at pilot and field scale. The mechanistic interpretations proposed here (electrostatic attraction, hydrogen bonding, π–π interactions, and pore-filling) are inferred from pH-dependence, FTIR, and thermodynamic data rather than confirmed by direct spectroscopic evidence; future work incorporating zeta potential measurements, pre- and post-adsorption FTIR or XPS analysis, and pilot-scale trials would help to substantiate the proposed adsorption mechanism and support scale-up.

Declarations

Funding

The research did not receive any funding

Author Contributions

Adamu, H.I.: Conceptualization, Methodology, Investigation, Formal analysis, Writing – original draft. Gbenga, A.A.: Methodology, Investigation, Writing review & editing. Yusuf, M.N.O.: Supervision, Validation, Writing – review & editing. All authors read and approved the final manuscript.

Competing Interests

The authors declare that they have no competing financial or non-financial interests in relation to this work.

Ethics, Consent to Participate, and Consent to Publish declarations: not applicable

Data Availability

The datasets generated and/or analysed during the current study are available from the corresponding author on reasonable request.

References

1. Jara-Cobos, L., Abad-Delgado, D., Ponce-Montalvo, J., Menendez, M., and Peñafiel, M. E. (2023). Removal of ciprofloxacin from an aqueous medium by adsorption on natural and hydrolyzed bentonites. Frontiers in Environmental Science.

2. Lunge, S., Singh, S., & Sinha, A. (2014). Magnetic iron oxide (Fe_3O_4) nanoparticles from tea waste for arsenic removal. *Journal of Magnetism and Magnetic Materials, 19*, 21–31. https://doi.org/10.1016/j.jmmm.2013.12.008.

3. Mohamed Khalith, S. B., Ramalingam, R., Karuppannan, S. K., Dowlath, M. J. H., Kumar, R., Vijayalakshmi, S., Uma Maheshwari, R., and Arunachalam, K. D. (2022). Synthesis and characterisation of polyphenols functionalized graphitic hematite nanocomposite adsorbent from an agro waste and its application for removal of Cs from aqueous solution. Chemosphere, 286(P1), 131493.

4. Adelere, I. A., & Lateef, A. (2016). Green synthesis of metallic nanoparticles: Plant-derived phytochemicals as reducing and stabilizing agents. *Biotechnology & Molecular Biology Reviews*, 11(1), 1–23.

5. Adegoke, H. I., & Gbenga, A. A. (2023). Bio-Assisted Synthesis of Zinc Oxide Nanoparticles from Mimosa pudica Aqueous Leave Extract: Structure and Antibacterial Activity. *Chemistry Africa*. https://doi.org/10.1007/s42250-022-00581-4.

6. Jamzad, M., & Kamari Bidkorpeh, M. (2020). Green synthesis of iron oxide nanoparticles by the aqueous extract of *Laurus nobilis* L. leaves and evaluation of the antimicrobial activity. *Journal of Nanostructure in Chemistry, 10*(3), 193–201.

7. Poh Yan, L., Gopinath, S. C., Subramaniam, S., Chen, Y., Velusamy, P., Chinni, S. V., ... & Lebaka, V. R. (2022). Greener synthesis of nanostructured iron oxide for medical and sustainable agro-environmental benefits. *Frontiers in Chemistry, 10*, 984218.

8. Hwang, N., & Barron, A. R. (2011). BET surface area analysis of nanoparticles. *The Connexions Project*, 1–11.

9. Bakatula, E. N., Richard, D., Neculita, C. M., & Zagury, G. J. (2018). Determination of point of zero charge of natural organic materials. *Environmental Science and Pollution Research, 25*, 7823–7833.

10. Plazinski, W., Dziuba, J., & Rudzinski, W. (2013). Modeling of sorption kinetics: The pseudo second order equation and the sorbate intraparticle diffusivity. *Adsorption, 19*, 1055–1064.

11. Wei, F., Wang, K., Li, W., Ren, Q., Qin, L., Yu, M., ... & Wang, S. (2023). Preparation of Fe/Ni MOFs for the adsorption of ciprofloxacin from wastewater. *Molecules, 28*(11), 4411.

12. Yew, Y. P., Shameli, K., Miyake, M., Kuwano, N., Bt Ahmad Khairudin, N. B., Bt Mohamad, S. E., and Lee, K. X. (2016). Green synthesis of magnetite (Fe_3O_4) nanoparticles using seaweed (Kappaphycus alvarezii) extract. Nanoscale Research Letters, 11(1), 1-7.

13. Stan et al., 2017 — full reference details for this in-text citation could not be located in the original reference list. Please verify the source and add the complete citation.

14. Baig, N., Kammakakam, I., & Falath, W. (2021). Nanomaterials: A review of synthesis methods, properties, recent progress, and challenges. *Materials Advances, 2*(6), 1821–1871.

15. Joudeh, N., & Linke, D. (2022). Nanoparticle classification, physicochemical properties, characterization, and applications: A comprehensive review for biologists. *Journal of Nanobiotechnology, 20*(1), 262.

16. Scrimieri, L., Velardi, L., Serra, A., Manno, D., Ferrari, F., Cantarella, M., & Calcagnile, L. (2020). Enhanced adsorption capacity of porous titanium dioxide nanoparticles synthetized in alkaline sol. *Applied Physics A, 126*, 1–8.

17. Reddy, M. S. B., Ponnamma, D., Sadasivuni, K. K., Kumar, B., & Abdullah, A. M. (2021). Carbon dioxide adsorption based on porous materials. *RSC Advances, 11*(21), 12658–12681.

18. Al-Musawi, T. J., Mahvi, A. H., Khatibi, A. D., & Balarak, D. (2021). Effective adsorption of ciprofloxacin antibiotic using powdered activated carbon magnetized by iron (III) oxide magnetic nanoparticles. *Journal of Porous Materials, 28*, 835–852.

19. Bachheti, R. K., Konwarh, R., Gupta, V., Husen, A., & Joshi, A. (2019). Green synthesis of iron oxide nanoparticles: Cutting edge technology and multifaceted applications. *Nanomaterials and Plant Potential*, 239–259.

20. Wei, Y., Wang, L., Li, H., Yan, W., & Feng, J. (2022). Synergistic fluoride adsorption by composite adsorbents synthesized from different types of materials—a review. *Frontiers in Chemistry, 10*, 900660.

21. Kollarahithlu, S. C., & Balakrishnan, R. M. (2019). Adsorption of ibuprofen using cysteine modified silane-coated magnetic nanomaterial. *Environmental Science and Pollution Research, 26*, 34117–34126.

22. Elshabrawy, S. O., Elhussieny, A., Taha, M. M., Pal, K., & Fahim, I. S. (2023). Wastewater treatment via sugarcane bagasse pulp. *International Journal of Environmental Science and Technology*, 1–12.

23. Vicente-Martínez, Y., Caravaca, M., Soto-Meca, A., & Solana-González, R. (2020). Magnetic core-modified silver nanoparticles for ibuprofen removal: An emerging pollutant in waters. *Scientific Reports, 10*(1), 18288.

24. Hanbali, G., Jodeh, S., Hamed, O., Bol, R., Khalaf, B., Qdemat, A., & Samhan, S. (2020). Enhanced ibuprofen adsorption and desorption on synthesized functionalized magnetic multiwall carbon nanotubes from aqueous solution. *Materials, 13*(15), 3329.

25. Bello, O. S., Alao, O. C., Alagbada, T. C., Agboola, O. S., Omotoba, O. T., & Abikoye, O. R. (2021). A renewable, sustainable and low-cost adsorbent for ibuprofen removal. *Water Science and Technology, 83*(1), 111–122.

26. Balarak, D., Mahvi, A. H., Shim, M. J., & Lee, S. M. (2021). Adsorption of ciprofloxacin from aqueous solution onto synthesized NiO: Isotherm, kinetic and thermodynamic studies. *Desalination and Water Treatment, 212*, 390–400.

27. Mehta, J., Dhaka, R. K., Dilbaghi, N., Lim, D. K., Hassan, A. A., Kim, K. H., & Kumar, S. (2022). Recent advancements in adsorptive removal of organophosphate pesticides from aqueous phase using nanomaterials. *Journal of Nanostructure in Chemistry*, 1–18.

28. Xing, X., Feng, J., Lv, G., Song, K., Mei, L., Liao, L., ... & Xu, B. (2015). Adsorption mechanism of ciprofloxacin from water by synthesized birnessite. *Advances in Materials Science and Engineering*, 2015.

29. Ali, A., Zafar, H., Zia, M., ul Haq, I., Phull, A. R., Ali, J. S., & Hussain, A. (2016). Synthesis, characterization, applications, and challenges of iron oxide nanoparticles. *Nanotechnology, Science and Applications*, 49–67.

30. Rafati, L., Ehrampoush, M. H., Rafati, A. A., Mokhtari, M., & Mahvi, A. H. (2018). Removal of ibuprofen from aqueous solution by functionalized strong nano-clay composite adsorbent: Kinetic and equilibrium isotherm studies. *International Journal of Environmental Science and Technology, 15*, 513–524.

31. Robati, D. (2013). Pseudo-second-order kinetic equations for modeling adsorption systems for removal of lead ions using multi-walled carbon nanotube. *Journal of Nanostructure Chemistry, 3*, 55.

32. Zeng, Z. W., Tan, X. F., Liu, Y. G., Tian, S. R., Zeng, G. M., Jiang, L. H., ... & Yin, Z. H. (2018). Comprehensive adsorption studies of doxycycline and ciprofloxacin antibiotics by biochars prepared at different temperatures. *Frontiers in Chemistry, 6*, 80.

33. Mutavdžić Pavlović, D., Ćurković, L., Grčić, I., Šimić, I., & Župan, J. (2017). Isotherm, kinetic, and thermodynamic study of ciprofloxacin sorption on sediments. *Environmental Science and Pollution Research, 24*, 10091–10106.

34. Qalyoubi, L., Al-Othman, A., Al-Asheh, S., Shirvanimoghaddam, K., Mahmoodi, R., & Naebe, M. (2023). Textile-based biochar for the removal of ciprofloxacin antibiotics from water. *Emergent Materials*, 1–12.

35. Sadegh, H., Ali, G. A., Gupta, V. K., Makhlouf, A. S. H., Shahryari-Ghoshekandi, R., Nadagouda, M. N., and Megiel, E. (2017). The role of nanomaterials as effective adsorbents and their applications in wastewater treatment. Journal of Nanostructure in Chemistry, 7, 1-14.

36. Rata, D. M., Cadinoiu, A. N., Daraba, O. M., Gradinaru, L. M., Atanase, L. I., & Ichim, D. L. (2023). Influence of ZnO nanoparticles on the properties of ibuprofen-loaded alginate based biocomposite hydrogels with potential antimicrobial and anti-inflammatory effects. *Pharmaceutics, 15*(9), 2240.

37. Moradi, S. E., Haji Shabani, A. M., Dadfarnia, S., & Emami, S. (2016). Effective removal of ciprofloxacin from aqueous solutions using magnetic metal-organic framework sorbents: Mechanisms, isotherms and kinetics. *Journal of the Iranian Chemical Society, 13*, 1617–1627.

38. Wakejo, W. K., Meshasha, B. T., Kang, J. W., & Chebude, Y. (2022). Enhanced ciprofloxacin removal from aqueous solution using a chemically modified biochar derived from bamboo sawdust: Adsorption process optimization with response surface methodology. *Adsorption Science and Technology*, 1–23.

39. Baratta, M., Tursi, A., Curcio, M., Cirillo, G., Nezhdanov, A. V., Mashin, A. I., ... & De Filpo, G. (2022). Removal of non-steroidal anti-inflammatory drugs from drinking water sources by GO-SWCNT buckypapers. *Molecules, 27*(22), 7674.

40. Alameri, A. A., Alfilh, R. H., Awad, S. A., Zaman, G. S., Al-Musawi, T. J., Joybari, M. M., ... & McKay, G. (2022). Ciprofloxacin adsorption using magnetic and ZnO nanoparticles supported activated carbon derived from *Azolla filiculoides* biomass. *Biomass Conversion and Biorefinery*, 1–14.

41. Campos, I., Espindola, A., Chagas, C., Barbosa, E., Castro, C. E., Molina, C., ... & Haddad, P. S. (2020). Biocompatible superparamagnetic nanoparticles with ibuprofen as potential drug carriers. *SN Applied Sciences, 2*, 1–12.

42. Rahimi, M., & Vadi, M. (2014). Adsorption of propranolol on multi-wall carbon nanotube. *International Journal of Advanced Biological and Biomedical Research, 2*(5), 1560–1564.

43. Gor, A. H., & Dave, P. N. (2020). Adsorptive abatement of ciprofloxacin using $NiFe_2O_4$ nanoparticles incorporated into *G. ghatti*-cl-P(AAm) nanocomposites hydrogel: Isotherm, kinetic, and thermodynamic studies. *Polymer Bulletin, 77*(11), 5589–5613.

44. Pulido-Díaz, I. T., Serrano-Maldonado, A., López-Suárez, C. C., Méndez-Ocampo, P. A., Portales-Martínez, B., Gutiérrez-Alejandre, A., ... & Guerrero-Ríos, I. (2021). RhNPs supported on N-functionalized mesoporous silica: Effect on catalyst stabilization and catalytic activity. *Dalton Transactions, 50*(9), 3289–3298.

45. Azizi, A. (2021). Green synthesis of iron oxide/cellulose magnetic recyclable nanocomposite and its evaluation in ciprofloxacin removal from aqueous solutions. Journal of the Iranian Chemical Society, 18(2), 331-341.

46. Edet, U. A., & Ifelebuegu, A. O. (2020). Kinetics, isotherms, and thermodynamic modeling of the adsorption of phosphates from model wastewater using recycled brick waste. *Processes, 8*(6), 665.

47. Kajjumba, G. W., Emik, S., Öngen, A., Özcan, H. K., & Aydın, S. (2018). Modelling of adsorption kinetic processes—errors, theory and application. *Advanced Sorption Process Applications*, 1–19.

48. Ebrahiminezhad, A., Zare-Hoseinabadi, A., Sarmah, A. K., Taghizadeh, S., Ghasemi, Y., & Berenjian, A. (2018). Plant-mediated synthesis and applications of iron nanoparticles. *Molecular Biotechnology, 60*, 154–168.

49. Mutia, A. S., Ariyanto, T., & Prasetyo, I. (2022). Ciprofloxacin removal from simulated wastewater through a combined process of adsorption and oxidation processes using Fe/C adsorbent. *Water, Air, and Soil Pollution, 233*(4), 146.

50. Shah, S. W. A., Rehman, M. U., Hayat, A., Tahseen, R., Bajwa, S., Islam, E., ... & Niazi, N. K. (2022). Enhanced degradation of ciprofloxacin in floating treatment wetlands augmented with bacterial cells immobilized on iron oxide nanoparticles. *Sustainability, 14*(22), 14997.

51. Masanabo, N., Orimolade, B., Idris, A. O., Nkambule, T. T., Mamba, B. B., & Feleni, U. (2023). Advances polymer-based detection of environmental ibuprofen wastewater. *Environmental Science and Pollution Research, 30*(6), 14062–14090.

52. Mohadesi, M., Gouran, A., & Seifi, K. (2022). Removal of ibuprofen from synthetic wastewater using photocatalytic method in the presence of FeO photocatalyst supported on modified Iranian clinoptilolite. *Environmental Science and Pollution Research, 29*(23), 34338–34348.

53. Ulvi, A., Aydın, S., & Aydın, M. E. (2022). Fate of selected pharmaceuticals in hospital and municipal wastewater effluent: Occurrence, removal, and environmental risk assessment. *Environmental Science and Pollution Research, 29*(50), 75609–75625.

54. Monteoliva-García, A., Martín-Pascual, J., Muñío, M. M., & Poyatos, J. M. (2019). Removal of carbamazepine, ciprofloxacin and ibuprofen in real urban wastewater by using light-driven advanced oxidation processes. *International Journal of Environmental Science and Technology, 16*(10), 6005–6018.

55. World Health Organization. (2012). *Pharmaceuticals in drinking-water*.

56. Silva, A. R., Gomes, J. C., Salvador, A. F., Martins, G., Alves, M. M., and Pereira, L. (2020). Ciprofloxacin, diclofenac, ibuprofen and 17α-ethinylestradiol differentially affect the

activity of acetogens and methanogens in anaerobic communities. Ecotoxicology, 29(7), 866-875.